Extension of the basin Rayleigh-wave amplification theory to include basin-edge effects

Quentin Brissaud, Daniel Bowden and Victor C. Tsai

This supplementary material aims at providing a more thorough description of the wavefield composition in semi-infinite basins and the spatial and frequency dependence of vertical and horizontal amplification spectra for semi-infinite and closed basins.

Wavefield composition in semi-infinite basins

In Section *Basin-edge velocity contrast and mode conversion*, we describe the Rayleigh-wave amplification spectra in basins with various basin-to-rock velocity ratios. In the main document, in Figures 2 and 3, we show that the propagation of the first overtone drastically changes the amplification spectrum. To confirm the presence of a first higher-order mode propagating from the basin edge, particle motions are a good way of distinguishing between various modes (Ma et al. 2016). Time series have been high-pass filtered, with corner frequency $f_c = 0.55$ Hz which corresponds to the basin dominant frequency, in order to clearly separate the fundamental and first overtones. In Figure S1 we show the particle motions corresponding to Figure 2 (a), where we observe an initial prograde wave motion (red background), expected for higher-order modes, followed by a larger retrograde wave motion (white background), expected for the fundamental mode. In Figure S2 we show the particle motions corresponding to Figure 2 (b). Note that the phase and group velocities corresponding to each of these examples are shown in Figure S3.

As described in Section *Lateral resonance*, the amplification spectrum is not only frequency dependent but also strongly dependent on the distance from the basin edge. To further examine the variations in amplification with distance from the basin edge for the examples presented in Figures 2 and 3, we show in Figures S4 (*b*) and S5 (*b*), respectively, the vertical and horizontal amplification spectra against distance from the basin edge extracted from the numerical simulations. We observe in Figures S4 (*a*) and S5 (*a*) a fast-propagating overtone, followed by a fundamental-mode Rayleigh wave. The overtone introduces oscillations in the amplification spectra presented in Figures in Figures S4 (*b*) and S5 (*b*). In Figures S6 and S7, we present similar results for a basin with $v_{0,basin} = 1.4$ km/s.

Finally, we note in Section *Basin-edge velocity contrast and mode conversion* that the horizontal and vertical local amplification maxima show a frequency shift. To explore the spatial dependence of this "out-of-phase" behavior, we show in Figure S8 the horizontal and vertical amplification spectra in panels (*b*) and (*c*) as well as their ratio (horizontal over vertical) against the distance from the basin edge (km) in panel (*a*) for a basin shear-velocity $v_{0,basin} = 1.2$ km/s. We observe in Figure S8 (*a*) that the frequency shift between horizontal and vertical local maxima reduces with increasing distance from the basin edge. In Figure S9, we present similar results for a basin with $v_{0,basin} = 1.4$ km/s.

Impact of reflections on the amplification spectrum

In Sections *Basin-edge velocity contrast and mode conversion* and *Lateral resonance* we describe the structure of the amplification spectrum in a closed basin where reflected Rayleigh waves interfere with incident Rayleigh waves. To further explore the impact of the reflected wavefield on the spatial-dependence of the amplification spectrum, we show in Figure S10 the ratio of vertical and horizontal amplification spectra in a basin with length $L_{basin} = 5$ km over amplification spectra in a semi-infinite basin, i.e. without reflection. We observe in Figure S10 that the maximum amplification variation ($\approx 10\%$) due to the reflected wavefield occurs for the vertical component close to the second basin edge around $f/f_h \approx 1.3$, i.e. around the first higher-order transmission coefficient peak frequency.

REFERENCES

Ma, Y., Clayton, R. W., & Li, D., 2016. Higher-mode ambient-noise rayleigh waves in sedimentary basins, *Geophysical Journal International*, **206**(3), 1634–1644.

LIST OF FIGURES

Figure S7 Panel (a), Normalized horizontal velocity against distance from the basin edge (km) and reduced time $t - t_0$ (s), with t_0 the time at which the incident wavetrain reaches the basin edge where $t_0 = 10.4$ s, for $h_{basin} = 1$ km, $v_{0,rock} = 2$ km/s and $v_{0,basin} = 1.4$ km/s. The color bar corresponds to the normalized horizontal velocity amplitude. Panel (b), the corresponding horizontal amplification against distance from the basin edge (km). The color bar corresponds to the horizontal amplification amplitude.

Figure S8 Panel (a), ratio of horizontal over vertical amplification spectra against normalized frequency and distance from the basin edge, for $h_{basin} = 1$ km and $v_{0,rock} = 2$ for $v_{0,basin} = 1.2$ km/s. The color bar corresponds to the ratio's value. Panels (b) and (c), the corresponding vertical and horizontal amplification spectra against normalized frequency and distance from the basin edge. The color bar corresponds to the amplification amplitude.

Figure S9 Panel (a), ratio of horizontal over vertical amplification spectra against normalized frequency and distance from the basin edge, for $h_{basin} = 1$ km and $v_{0,rock} = 2$ for $v_{0,basin} = 1.4$ km/s. The color bar corresponds to the ratio's value. Panels (b) and (c), the corresponding vertical and horizontal amplification spectra against normalized frequency and distance from the basin edge. The color bar corresponds to the amplification amplitude.

Figure S10 Ratio of amplification spectra in a basin with length $L_{basin} = 5$ km over amplification spectra in a semi-infinite basin, i.e. without reflection against relative location for the vertical component (panel (a)) and the horizontal component (panel (b)).

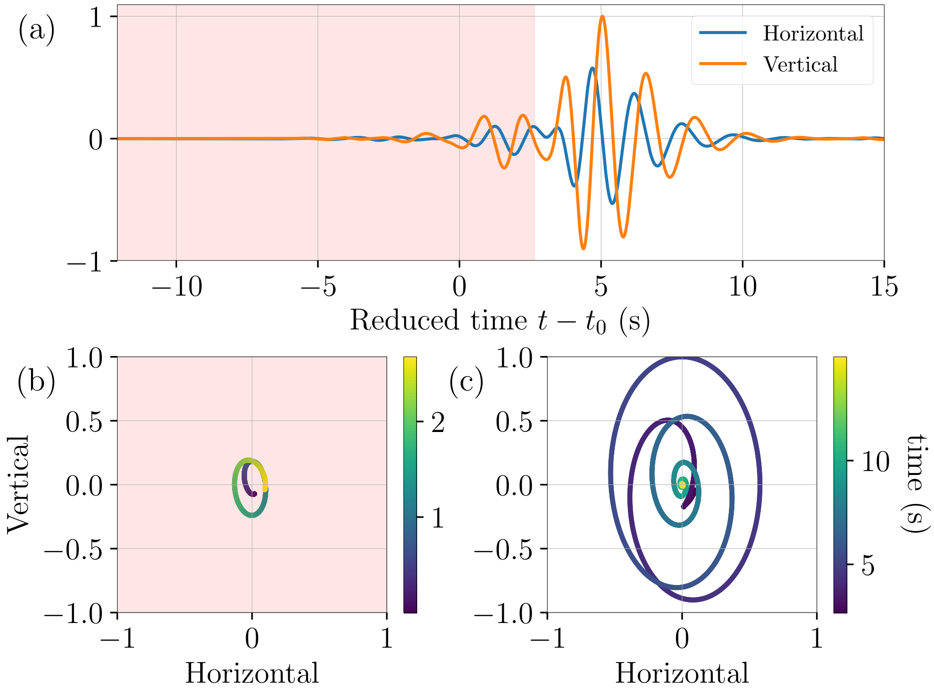

Figure S1. Panel (a), normalized high-pass filtered (corner frequency $f_c = 0.55$ Hz) velocity (m/s) against reduced time $t - t_0$ (s), with t_0 the time at which the incident wavetrain reaches the basin edge where $t_0 = 12$ s, for the horizontal component (blue) and the vertical component (orange) corresponding to Figure 2 (a) at distance $x = 5$ km from the basin edge, for $h_{basin} = 1$ km, $v_{0,rock} = 2$ and $v_{0,basin} = 1.2$ km/s. Panels (b) and (c) show the particle motions, in terms of horizontal and vertical velocities, associated with the signal highlighted by, respectively, the red and white backgrounds in panel (a). The color bar shows the corresponding reduced time $t - t_0$ (s).

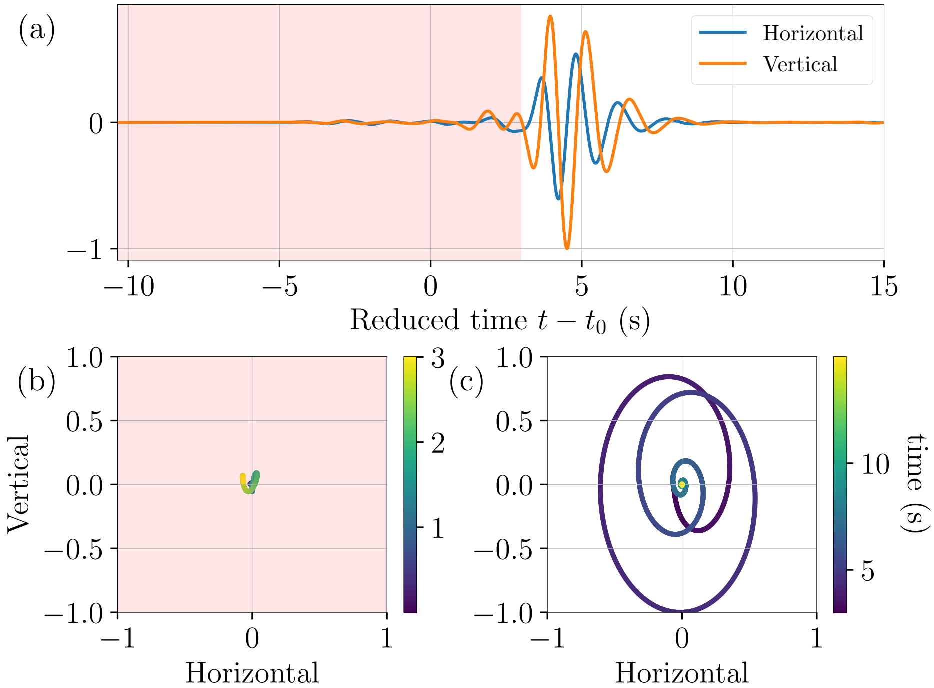

Figure S2. Panel (a), normalized high-pass filtered (corner frequency $f_c = 0.6$ Hz) velocity (m/s) against reduced time $t - t_0$ (s), with t_0 the time at which the incident wavetrain reaches the basin edge where $t_0 = 10.4$ s, for the horizontal component (blue) and the vertical component (orange) corresponding to Figure 2 (b) at distance $x = 5$ km from the basin edge, for $h_{basin} = 1$ km, $v_{0,rock} = 2$ and $v_{0,basin} = 1.4$ km/s. Panels (b) and (c) show the particle motions, in terms of horizontal and vertical velocities, associated with the signal highlighted by, respectively, the red and white backgrounds in panel (a). The color bar shows the corresponding reduced time $t - t_0$ (s).

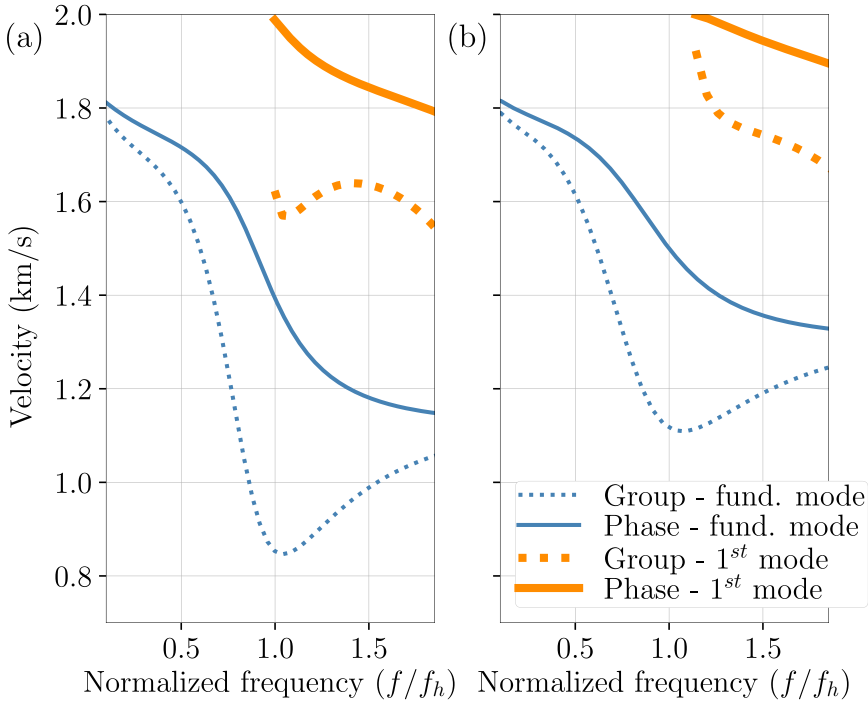

Figure S3. Rayleigh-wave group (dashed) and phase (solid) velocities for the fundamental mode (blue) and the first higher-order mode (orange) against normalized frequency for a basin with $h_{basin} = 1$ km, $v_{0,rock} = 2$ km/s and $v_{0,basin} = 1.2$ km/s (panel (a)) or $v_{0,basin} = 1.4$ km/s (panel (b)).

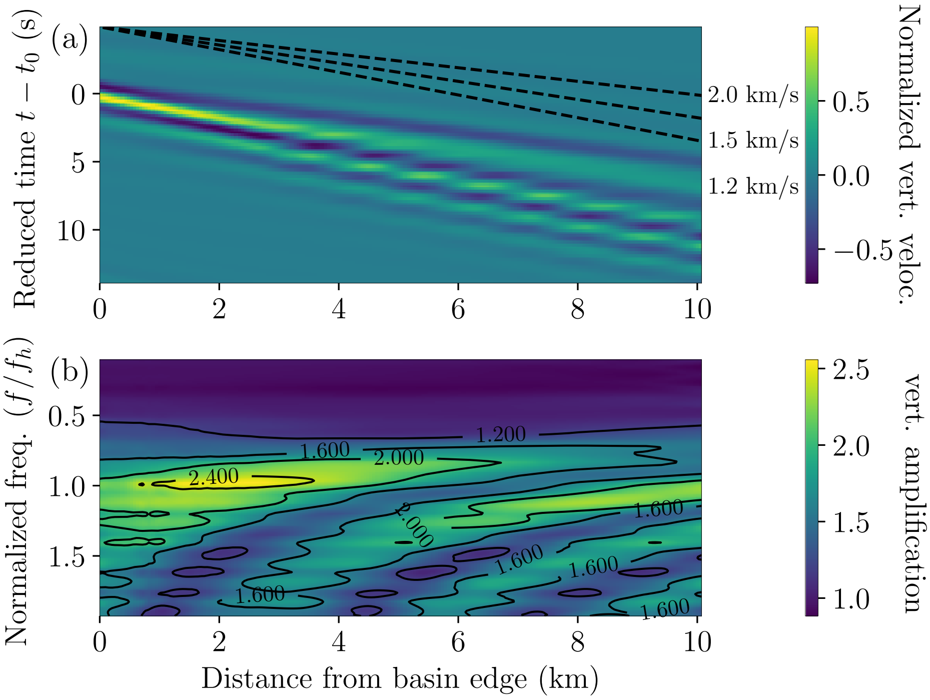

Figure S4. Panel (a), Normalized vertical velocity against distance from the basin edge (km) and reduced time $t - t_0$ (s), with t_0 the time at which the incident wavetrain reaches the basin edge where $t_0 = 12$ s, for $h_{basin} = 1$ km, $v_{0,rock} = 2$ km/s and $v_{0,basin} = 1.2$ km/s. The color bar corresponds to the normalized vertical velocity amplitude. Panel (b), the corresponding vertical amplification against distance from the basin edge (km). The color bar corresponds to the vertical amplification amplitude.

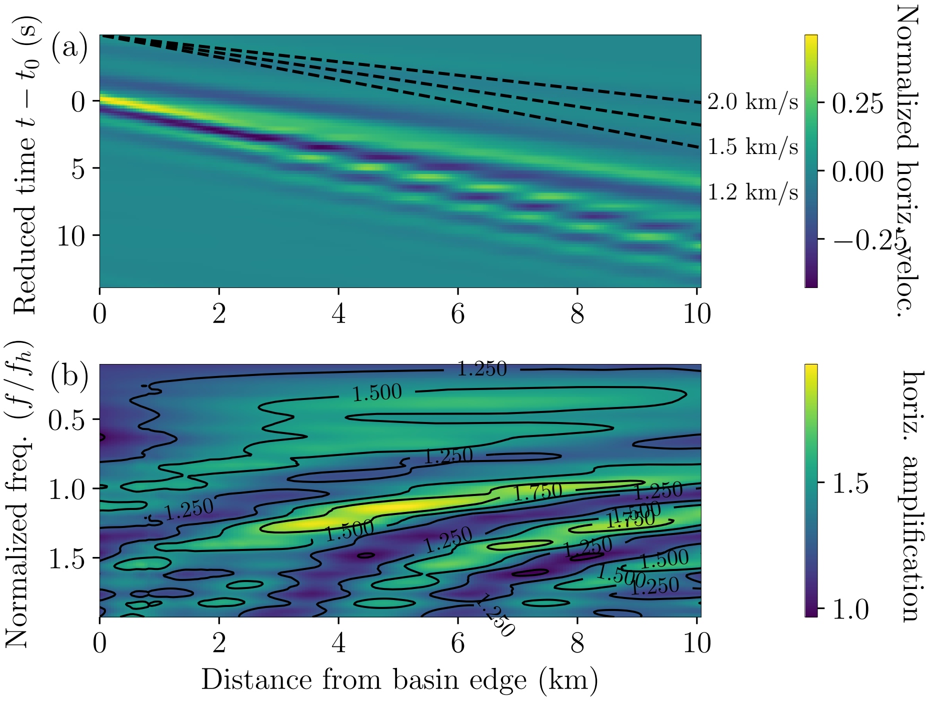

Figure S5. Panel (a), Normalized horizontal velocity against distance from the basin edge (km) and reduced time $t - t_0$ (s), with t_0 the time at which the incident wavetrain reaches the basin edge where $t_0 = 12$ s, for $h_{basin} = 1$ km, $v_{0,rock} = 2$ km/s and $v_{0,basin} = 1.2$ km/s. The color bar corresponds to the normalized horizontal velocity amplitude. Panel (b), the corresponding horizontal amplification against distance from the basin edge (km). The color bar corresponds to the horizontal amplification amplitude.

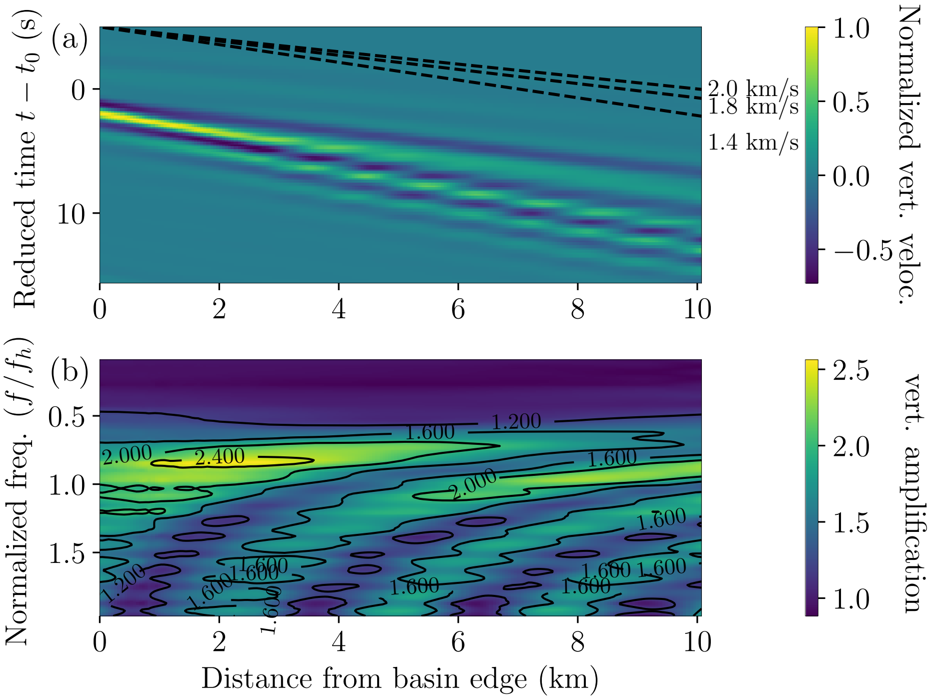

Figure S6. Panel (a), Normalized vertical velocity against distance from the basin edge (km) and reduced time $t - t_0$ (s), with t_0 the time at which the incident wavetrain reaches the basin edge where $t_0 = 10.4$ s, for $h_{basin} = 1$ km, $v_{0,rock} = 2$ km/s and $v_{0,basin} = 1.4$ km/s. The color bar corresponds to the normalized vertical velocity amplitude. Panel (b), the corresponding vertical amplification against distance from the basin edge (km). The color bar corresponds to the vertical amplification amplitude.

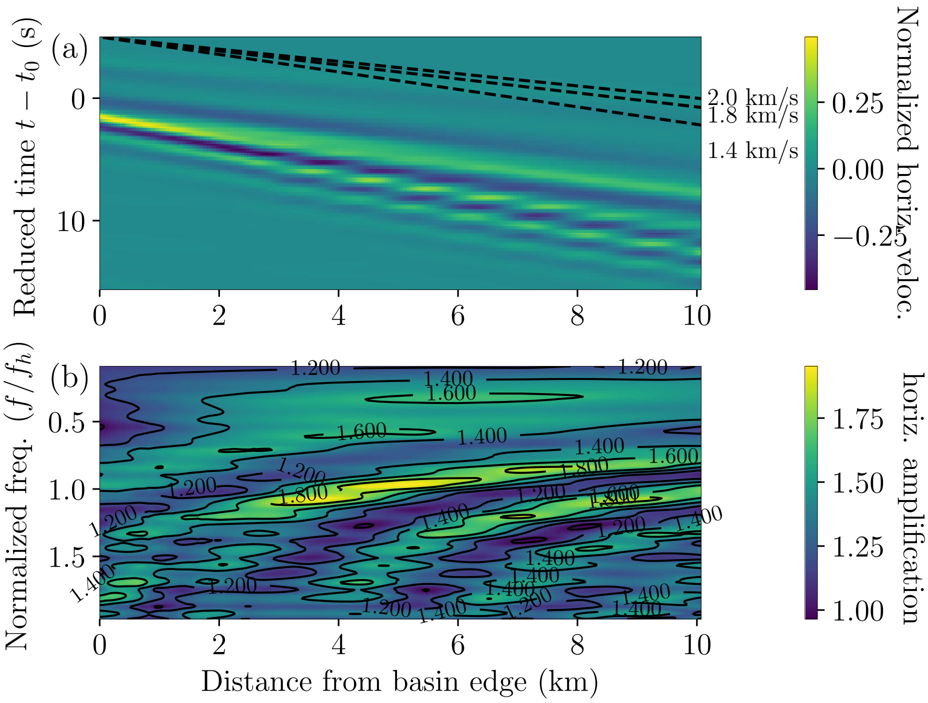

Figure S7. Panel (a), Normalized horizontal velocity against distance from the basin edge (km) and reduced time $t - t_0$ (s), with t_0 the time at which the incident wavetrain reaches the basin edge where $t_0 = 10.4$ s, for $h_{basin} = 1$ km, $v_{0,rock} = 2$ km/s and $v_{0,basin} = 1.4$ km/s. The color bar corresponds to the normalized horizontal velocity amplitude. Panel (b), the corresponding horizontal amplification against distance from the basin edge (km). The color bar corresponds to the horizontal amplification amplitude.

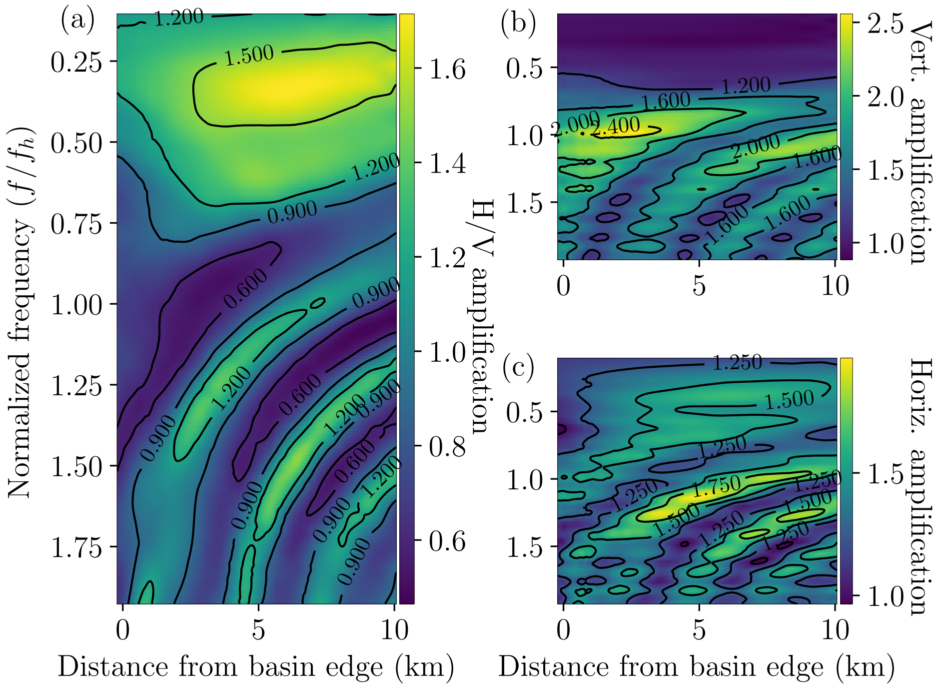

Figure S8. Panel (a), ratio of horizontal over vertical amplification spectra against normalized frequency and distance from the basin edge, for h_{basin} = 1 km and $v_{0,rock}$ = 2 for $v_{0,basin}$ = 1.2 km/s. The color bar corresponds to the ratio's value. Panels (b) and (c), the corresponding vertical and horizontal amplification spectra against normalized frequency and distance from the basin edge. The color bar corresponds to the amplification amplitude.

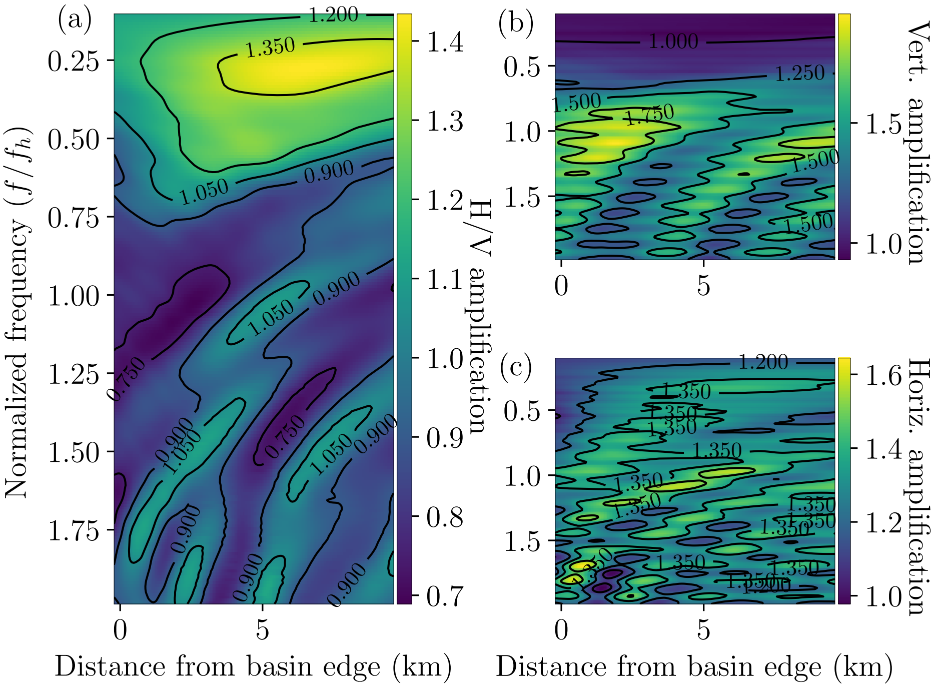

Figure S9. Panel (a), ratio of horizontal over vertical amplification spectra against normalized frequency and distance from the basin edge, for h_{basin} = 1 km and $v_{0,rock}$ = 2 for $v_{0,basin}$ = 1.4 km/s. The color bar corresponds to the ratio's value. Panels (b) and (c), the corresponding vertical and horizontal amplification spectra against normalized frequency and distance from the basin edge. The color bar corresponds to the amplification amplitude.

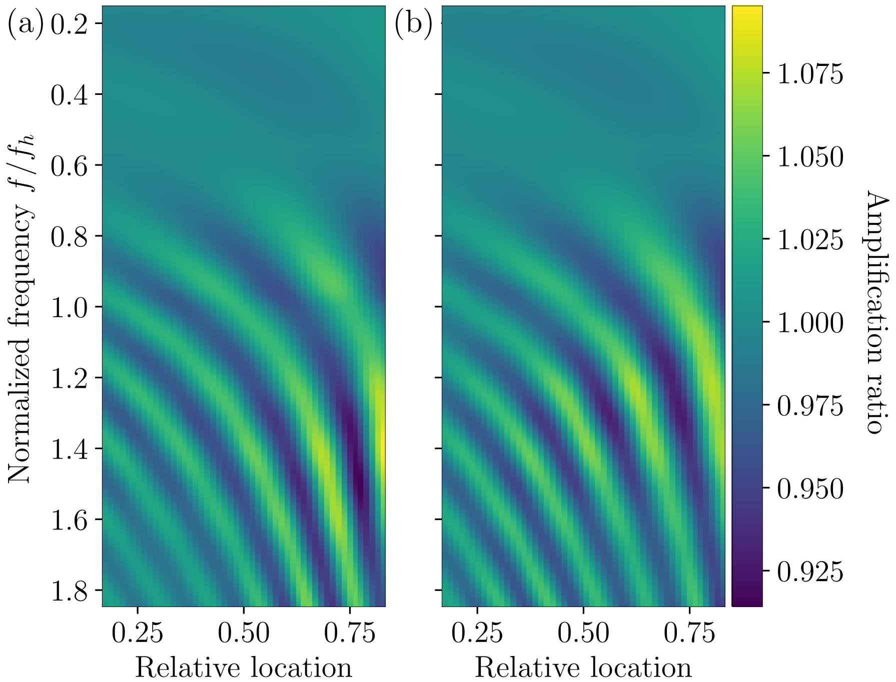

Figure S10. Ratio of amplification spectra in a basin with length $L_{basin} = 5$ km over amplification spectra in a semi-infinite basin, i.e. without reflection against relative location for the vertical component (panel (a)) and the horizontal component (panel (b)).